

Prep1 (pKnox1) transcription factor contributes to pubertal mammary gland branching morphogenesis

LARA SICOURI¹, FEDERICA PISATI¹, SALVATORE PECE^{2,3}, FRANCESCO BLASI^{*,1} and ELENA LONGOBARDI^{*,1,4}

¹IFOM (FIRC Institute of Molecular Oncology), Milan, ²Department of Experimental Oncology, European Institute of Oncology, Milan, ³Department of Oncology and Hemato-Oncology, University of Milan, Milan, and ⁴Section of Pharmacology, Department of Neuroscience, University of Naples Federico II, Naples, Italy

ABSTRACT Prep1 (pKnox1) is a homeodomain transcription factor essential for *in utero* and post-natal development and an oncosuppressor gene in human and adult mice. We have analyzed its role in the development of the mouse mammary gland. We used *Prep1^{i/i}* hypomorphic and *Prep1^{F/F}-Ker5CRE* crosses to analyze the role of Prep1 *in vivo* in adult mouse mammary gland development. We also cultured mammary gland stem/progenitor cells in mammospheres to perform biochemical studies. Prep1 was expressed in mammary gland progenitors and fully differentiated mammary gland cells. Using different *Prep1*-deficient mouse models we show that *in vivo* Prep1 contributes to mammary gland branching since the branching efficiency of the mammary gland in *Prep1*-deleted or *Prep1* hypomorphic mice was largely reduced. *In-vitro*, *Prep1* sustained functions of the mammary stem/progenitor compartment. *Prep1*-deficient mammary stem/progenitor cells showed reduced ability to form mammospheres; they were not able to branch in a 3D assay, and exhibited reduced expression of *Snail1*, *Snail2* and vimentin. The branching phenotype associated with increased *Tp53*-dependent apoptosis and inability to properly activate signals involved in branching morphogenesis. Finally, Prep1 formed complexes with Snail2, a transcription factor essential in branching morphogenesis, and its absence destabilizes and promotes Snail2 proteasome-mediated degradation. We conclude that *Prep1* is required for normal adult mammary gland development, in particular at its branching morphogenesis step. By binding Snail2, Prep1 protects it from the proteasomal degradation.

KEY WORDS: *prep1*, mammary gland, mammosphere, branching morphogenesis, transcription factor, apoptosis



Introduction

Prep1 (pKnox1) homeodomain transcription factor belongs to the TALE (Three Amino acids Loop Extension) superclass of proteins that also include Meis and Pbx (Longobardi *et al.*, 2014). Prep1 and Pbx1 are essential during embryonic development and are required for organogenesis and differentiation (Selleri *et al.*, 2001; Ferretti *et al.*, 2006; Fernandez-Diaz *et al.*, 2010). Prep1 is ubiquitously expressed both in developing and adult mice and regulates transcription by binding mostly promoters, preferentially together with Pbx1 (Penkov *et al.*, 2013). Importantly, Prep1-Pbx dimerization regulates their subcellular localization, Pbx stability and DNA selectivity (Berthelsen *et al.*, 1999; Longobardi and Blasi,

2003; Penkov *et al.*, 2013).

In zebrafish embryos, down-regulation of Prep1.1 causes diffuse apoptosis, hindbrain and craniofacial deficiencies and embryonic

Abbreviations used in this paper: CHX, cycloheximide; CRE, cyclization recombinase; CT, carboxyterminal; EMT, epithelial to mesenchymal transition; HD, homeodomain; HE, hematoxylin-eosin; IF, immunofluorescence; IHC, immunohistochemistry; MaSC, mammary stem cell; MEC, mammary epithelial cell; Pbx, Pre-B cell leukemia transcription factor; p-EMT partial EMT; Prep1 (pKnox1). Pbx-regulating protein 1; RT-PCR, reverse transcription-polymerase chain reaction; SFE, mammosphere forming efficiency; shRNA, short hairpin RNA; SMA, smooth muscle actin; TALE, three amino acids loop extension; TEB, terminal end bud.

*Address correspondence to: Elena Longobardi. Section of Pharmacology, Department of Neuroscience, University of Naples Federico II, Via S. Pansini 5, 80131 Naples, Italy. Tel: 081-7463316. Fax: 081-7463323. E-mail: elelong@libero.it -  <https://orcid.org/0000-0001-8283-4735> or Francesco Blasi. IFOM (FIRC Institute of Molecular Oncology), Via Adamello 16, 20139 Milan, Italy. Tel: 0039-02-574303288. Fax: 0039-02-574303222. E-mail: francesco.blasi@ifom.eu - web: <http://www.ifom.eu/en/cancer-research/research-labs/research-lab-blasi.php> -  <https://orcid.org/0000-0001-9406-1784>

Supplementary Material (6 figures and 2 tables) for this paper is available at: <https://doi.org/10.1387/ijdb.180278fb>

Submitted: 27 August, 2018. Accepted: 13 September, 2018.

lethality (De Florian *et al.*, 2004); in mouse, *Prep1*-null embryos undergo *Tp53*-dependent apoptosis of epiblast cells and developmental arrest before gastrulation (Fernandez-Diaz *et al.*, 2010). Mouse embryos carrying an hypomorphic *Prep1^{hi}* mutation caused by the insertion of a splice site within the first intron of the gene and expressing only 2% mRNA and 3-7% protein with respect to WT, show 75% embryonic lethality at E17.5 due to major alterations in hematopoiesis; moreover, angiogenesis and lens/retinogenesis defects are observed with lower penetrance (Ferretti *et al.*, 2006). The surviving 25% *Prep1^{hi}* mice display a broad range of phenotypes, namely T-cell differentiation defects, impaired folliculogenesis, alteration of glucose and lipid metabolism (Longobardi *et al.*, 2014). Moreover, cultured down-regulated mouse *Prep1^{hi}* embryonic and human *PREP1* fibroblasts accumulate double strand breaks and bypass oncogene-induced senescence, in the presence of an apparently functional DNA repair (Iotti *et al.*, 2011). This is due to anomalies in the timing of DNA replication and loss of DNA replication symmetry (Palmigiano *et al.*, 2018). In fact *Prep1* is a tumor suppressor: in mice the *Prep1^{hi}* mutants develop tumors at high frequency and in humans 75% of over 1,400 tumors show a major reduction of *PREP1* expression (Longobardi *et al.*, 2010). *PREP1* also affects cell migration function, since its overexpression hijacks the *TGF β* pathway inducing EMT (Epithelial-Mesenchymal Transition) in lung adenocarcinoma increasing the risk of metastasis (Risolino *et al.*, 2014).

At the molecular level, *Prep1* binds DNA as a dimer with *Pbx1* (Longobardi *et al.*, 2014). However, the dimer can also bind *HoxB1* and possibly other anterior *Hox* proteins, since *Prep1* interaction

occurs with the *Pbx* moiety and is not alternative to that of *Pbx* with *Hox*. In this respect it has been shown that the ternary *Prep1*-*Pbx1*-*HoxB1* complexes can bind the *HoxB1*, *HoxA2* enhancer regions and affect the expression of these *Hox* genes (Ferretti *et al.*, 2000). Indeed, in *D. rerio*, *Prep1.1* down-regulation results in a shut-off of the expression of several anterior *HoxB* genes in the hindbrain (De Florian *et al.*, 2004).

Post-natal mammary gland develops through a process known as branching morphogenesis, whereby the epithelial bud extends into the fat pad and bifurcates to form an extensive ductal network (Affolter *et al.*, 2003). Terminal End Buds (TEBs), located at the tip of the elongating ducts, sustain this process by providing mammary gland stem/progenitor cells (MaSC) (Paine and Lewis, 2017).

We now report that *Prep1* is expressed in differentiated ducts as well as in TEBs of the pre-pubertal mouse mammary gland and that its down-regulation, by multiple approaches, limits ducts branching. We also report that *Prep1* function extends to the MaSC/progenitor compartment in which it sustains cell viability and branching differentiation, through a mechanisms that includes apoptosis and modulation of components of the partial EMT process.

Results

Prep1 is expressed in mammary gland epithelial cells

To bypass estral cycle influence on the mammary gland development, we have used in the majority of cases only pre-pubertal (4-5 weeks old) animals: older animals have been sometimes used (and indicated) to confirm the results obtained with younger ones.

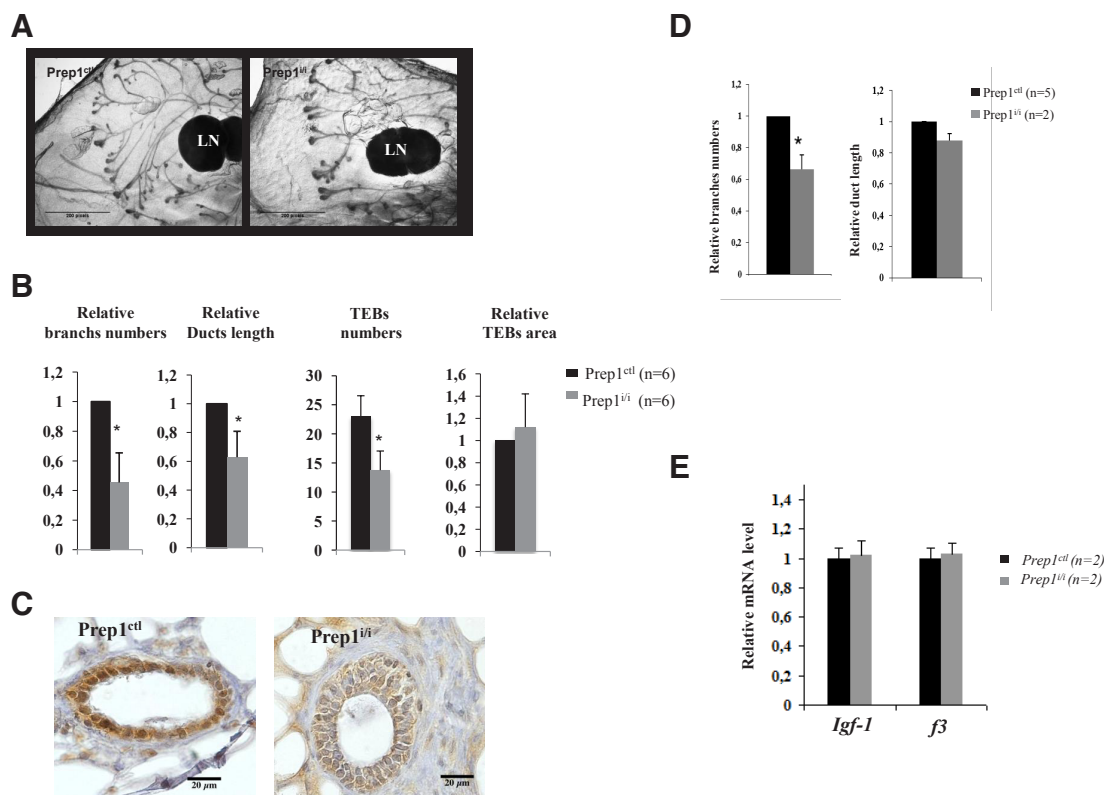


Fig. 1. *Prep1^{hi}* mice show major defects in branching morphogenesis. (A) Representative images of Carmine Alum-stained whole-mount preparations of mammary glands from 4-5 weeks-old virgin *Prep1^{hi}* female and age matched littermate control (*Prep1^{cti}*) mice. LN: lymph nodes. (B) Quantification of the major structural features of the epithelial tree (branch numbers, ducts length, TEB numbers and area) observed in *Prep1^{hi}* (*n*=6) as compared to *Prep1^{cti}* (*n*=6) glands. Detailed informations on quantifications are reported in Materials and Methods. Error bars indicate s.d. (**P* < 0.01). (C) IHC with *Prep1*-specific antibody confirms the strong reduction of *Prep1* signal in *Prep1^{hi}* glands. Scale bars: 20

μm . (D) The histograms report the morphological quantifications of ductal length and branch number on mammary gland obtained from 11-13 weeks old virgin *Prep1^{hi}* (*n* = 2) and *Prep1^{cti}* (*n*=5) mice. (**P*<0.05). (E) Q-PCR on mammary epithelial cells from controls (*Prep1^{cti}*) and *Prep1* hypomorphic (*Prep1^{hi}*) 5 weeks old mice. *Igf-1* and *f3* transcripts levels were evaluated. Numbers in brackets represent animals used for each genotype. Error bars show the s.d.

Immunofluorescence (IF) with a specific monoclonal antibody was used to localize Prep1 in the gland compartments of 4-5 weeks old virgin WT C57BL/6 mouse females. Specific staining for Prep1 was present in the epithelial and stromal cells (Fig. S1A, supplementary material). HE staining of the same section is also shown (Fig. S1B). Double IF with a α -Smooth Muscle Actin (SMA) antibody, specific for the basal myoepithelial cells, revealed that Prep1 was mainly nuclear in SMA-positive myoepithelial and stromal cells but stained both nucleus and cytoplasm in luminal cells (Fig. S1 C,D in supplementary material). A similar pattern of expression was observed for Pbx1 (Fig. S1 E,F) the major transcriptional partner of Prep1 (Penkov *et al.*, 2013). The presence of Prep1 in the cytoplasm may reflect either an excess over Pbx1 (since the latter transports it into the nucleus) (Berthelsen *et al.*, 1999) or represent different stages of an unknown regulatory mechanism.

***Prep1* deficient females display defective mammary gland morphogenesis**

To assess the importance of Prep1 in pre-pubertal mammary gland development, we used the hypomorphic *Prep1^{hi}* mice. These mice were generated by insertion of a splice-site containing vector in the first intron of the *Prep1* gene almost totally eliminating the WT Prep1 mRNA transcript, leaving only a residual 2-3% and about 7% of the protein (Ferretti *et al.*, 2006). Whole-mounts of inguinal glands were prepared from 4-5 weeks-old control and *Prep1^{hi}* virgin females and stained over night in Carmine Alum solution. A representative image is shown in Fig. 1A. Quantitative analysis (Fig. 1B) shows a statistically significant reduction of branching (nearly 60%) and of ducts length (nearly 40%) in *Prep1^{hi}*

compared to control glands. In addition, we found a statistically significant reduction of the number of TEBs, but not of the TEBs area. Immunohistochemistry (IHC) with Prep1 specific antibody on paraffin-embedded mammary gland sections confirmed the reduction of Prep1 signal in *Prep1^{hi}* female glands (Fig. 1C).

To assess whether the morphological defects observed in Prep1 deficient mouse models persisted at later developmental stages, we extended our analysis to 11-13 weeks old virgin control and *Prep1^{hi}* females. Morphological quantifications, reported in the histograms in Fig. 1D, showed that at this developmental stage *Prep1^{hi}* duct length defect was no longer significant and hence mammary glands were as efficient as control glands to reach the limit of the fat pad; however, *Prep1^{hi}* glands still showed a significant impairment in branching morphogenesis.

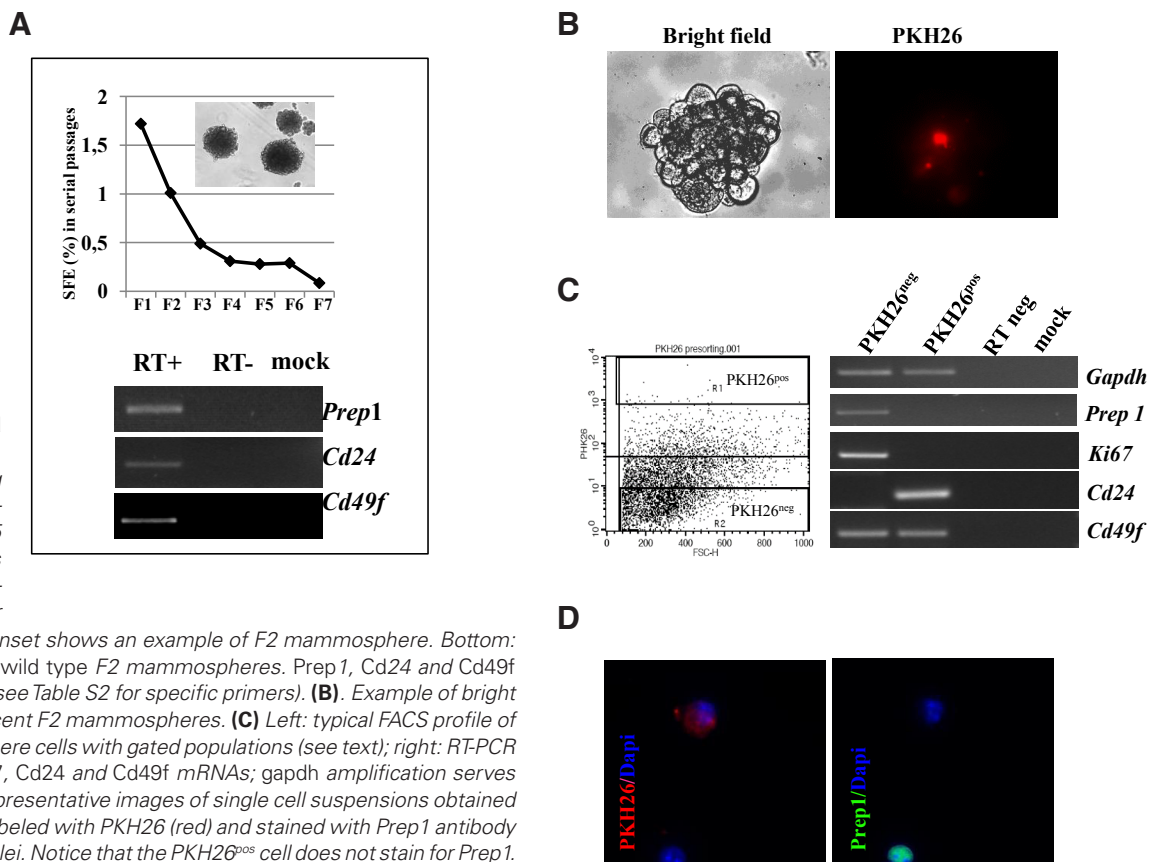
At the onset of puberty, growth hormone (GH) and estrogen (E2) sustain TEBs formation and branching morphogenesis (Paine and Lewis, 2017). To exclude that the branching phenotypes in Prep1 deficient mice might depend on aberrant hormonal responses, we tested *Prep1^{hi}* and *Prep1^{ctrl}* mammary epithelial cells for *Igf-1* and *F3* mRNAs levels, downstream targets of GH and estrogen respectively (Kleinberg, 1998). The results, reported in Fig. 1E, revealed that *Prep1^{hi}* epithelial cells expressed the same level of *Igf-1* and *F3* transcripts as control cells.

The branching phenotype was further confirmed by crossing a conditional *Prep1^{flxed}* mouse (Iotti *et al.*, 2012), with the *Ker5^{Cre}*-transgenic, in which the CRE activity (Ramirez *et al.*, 2004), and hence *Prep1* deletion, is restricted to the basal cells of stratified epithelia (not shown). Upon *Prep1* deletion, ducts branching was significantly affected; however, the difference in TEB numbers did

Fig. 2. *Prep1* is expressed in mouse mammospheres.

(A) Top: SFE in re-plating experiments using mammary epithelial cells from 5 weeks-old C57BL/6 females cultured in sphere-promoting conditions. F1...F7 refer to the serial replating. The inset shows an example of F2 mammosphere. Bottom:

RT-PCR on total RNA from wild type F2 mammospheres. *Prep1*, *Cd24* and *Cd49f* transcripts were analysed (see Table S2 for specific primers). (B). Example of bright field and PKH26 epifluorescent F2 mammospheres. (C) Left: typical FACS profile of PKH26-labeled mammosphere cells with gated populations (see text); right: RT-PCR amplification of *Prep1*, *Ki67*, *Cd24* and *Cd49f* mRNAs; *gapdh* amplification serves as a loading control. (D) Representative images of single cell suspensions obtained from F2 mammospheres labeled with PKH26 (red) and stained with *Prep1* antibody (green). DAPI stains the nuclei. Notice that the PKH26^{pos} cell does not stain for *Prep1*.



not reach statistical significance (Fig. S2 A,B in the supplementary material). Residual *Prep1* mRNA in mammary epithelial cells (MEC), evaluated by RT-PCR amplifications, was not observed (supplementary Fig. S2C).

Prep1 is expressed in mammary progenitor cells

At puberty, with their pool of stem/progenitor cells, the TEBs represent the major structures driving ductal elongation and branching (Paine and Lewis, 2017; Scheele et al., 2017). We wondered whether down-regulation of *Prep1* perturbed the mammary gland stem cell (MaSCs) niche within TEBs.

MaSCs can be cultured and propagated *in-vitro*, for at least 5-6 passages, under conditions promoting the formation of floating mammospheres. These are made up of a single, quiescent, mammary stem cell and many proliferating progenitors (Scheele et al., 2017). Using standard mammosphere-culturing conditions (see Methods) the spheres were propagated till the sixth (F6) serial passage (Fig. 2A). Evaluation of *Prep1* expression in second passage (F2) mammospheres (insert, Fig. 2A) by RT-PCR shows a specific amplified band for *Prep1*; amplification of *Cd49f* and *Cd24* mRNAs (Fig. 2A), two markers of mammary stem and progenitor cells (Stingl et al., 2006), confirms that the mammospheres contain

mammary stem and progenitor cells. Immunofluorescence on F2 mammospheres (Supplementary Fig. S3) confirms the presence of *Prep1* in most mammosphere cells and its preferential nuclear localization; likewise, also *Pbx1*, partner of *Prep1* in DNA binding, is expressed in the mammospheres. *Prep1* distribution within the mammosphere was further investigated using PKH26 labeling, by which the quiescent MaSCs can be identified because they are able to retain the dye, unlike progenitor cells that divide and therefore dilute it (Pece et al., 2010). Mammary epithelial cells from 4-5 weeks old C57BL/6 mice were collected, stained with the lipophilic dye PKH26 and plated to form mammospheres. After two serial replating only few cells inside the F2 mammospheres retained the PKH26 epifluorescent signal (Fig. 2B), as expected. F2 mammospheres were collected and single cell suspensions used to differentially FACS-separate the most epifluorescent 0.2%–0.4% of the total cell population (PKH^{pos} cells, gated at 10^3 – 10^4 fluorescence units), from the PKH^{neg} proliferating, lineage-committed, progenitors (gated at 10^0 – 10^1 fluorescence units) (Fig. 2C, left). Total RNA was extracted and used in RT-PCR (Fig. 2C, right) to assess the presence of *Prep1* mRNA in these two cell populations. A *Prep1* positive band was found in the PKH26^{neg} but not in the PKH26^{pos} population. Amplification of a band corresponding to *CD24* and *CD49f* but not of *Ki67* transcripts confirmed that the PKH^{pos} fraction was enriched in quiescent MaSC, as expected (Pece et al., 2010). The absence of *Prep1* in the PKH26^{pos} cells was further confirmed by double immunofluorescence: PKH26^{pos} cells did not stain for *Prep1*, unlike PKH26^{neg} cells (Fig. 2D). We conclude therefore that *Prep1* is expressed in the PKH26^{neg} progenitors population of the mammospheres.

We also evaluated the effect of *Prep1* down-regulation on the mammary stem activity measuring the Sphere Forming Efficiency (SFE) (Shaw et al., 2012) upon replating in two different *Prep1* down-regulated models: the hypomorphic *Prep1^{if}* and the wt mam-

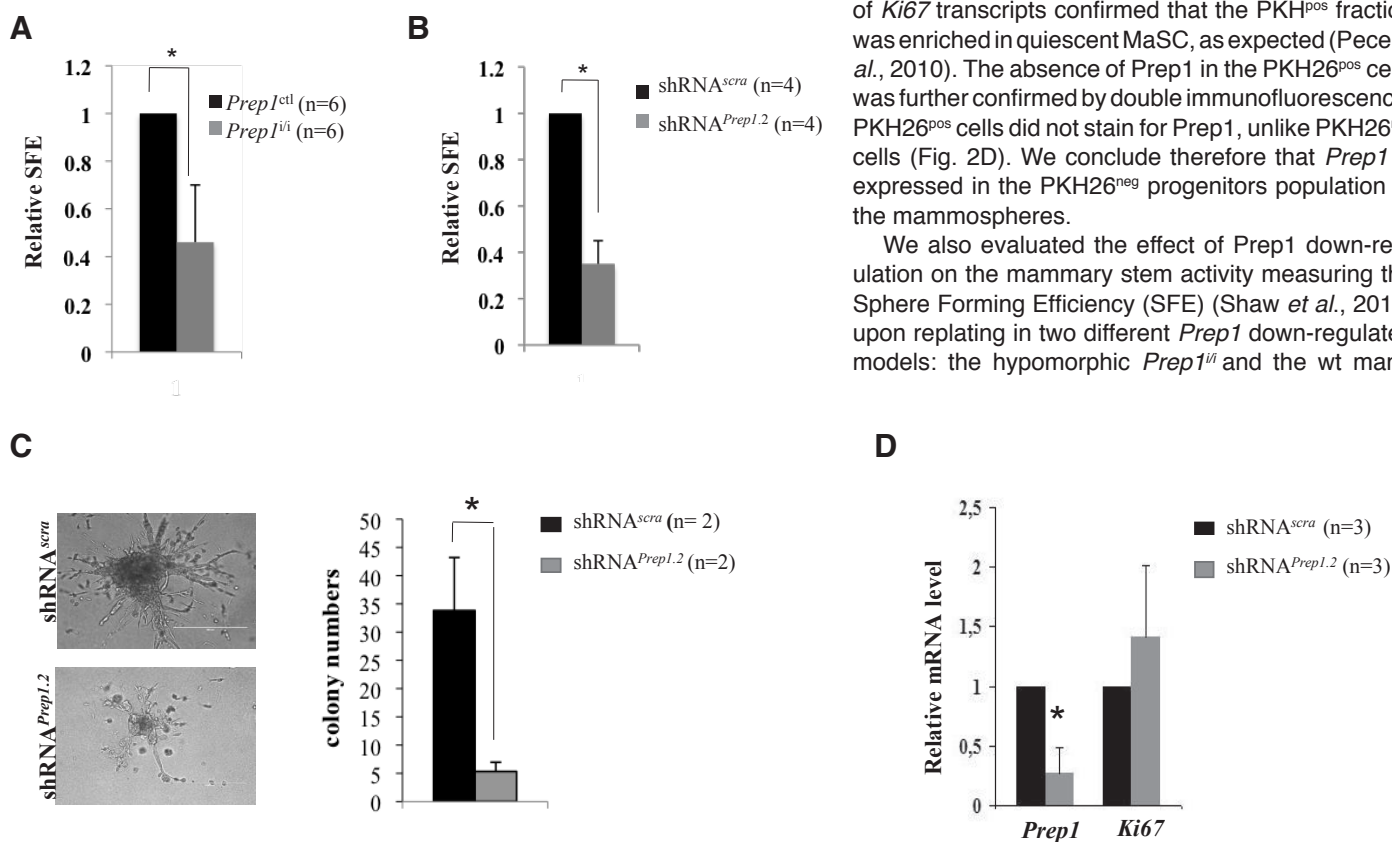


Fig. 3. *Prep1*-deficient MaSC/progenitors have a compromised Sphere Forming Efficiency (SFE). Purified MEC from *Prep1^{if}* and *Prep1^{ctrl}* glands (A) and WT MEC transduced with shRNA^{scra} or shRNA^{Prep1.2} lentiviruses (B) were seeded in low-adherence plates and grown as mammospheres. The SFE at passage 2 (F2) was evaluated. The number of animals (A) and the number of interference experiments (B) used for each experimental model is indicated in brackets, (* P < 0.001). Bars show the s.d. (C) *In-vitro* branching potential of *Prep1* deficient cells. MEC were infected with shRNA^{Prep1.2} or shRNA^{scra} viral supernatants and seeded in low-adherence plates and grown as mammospheres. After selection, the F2 cells were plated in Matrigel and cultured for 3 weeks for colony formation. Example of 3D colonies is shown on the left. Scale bar: 400 μ m. Quantification of colony number is reported in the histogram. Data refer to two independent experiments, each performed in triplicate. Bars indicate the s.d. (*P < 0.001). (D) Total RNA from F2 mammosphere cells interfered with shRNA^{Prep1.2} or shRNA^{scra} viral supernatants was retrotranscribed and cDNA used to amplify *Prep1* and *Ki67* mRNAs. Data refer to three independent interference experiments, each in triplicate. Bars show the s.d.; * p<0,01.

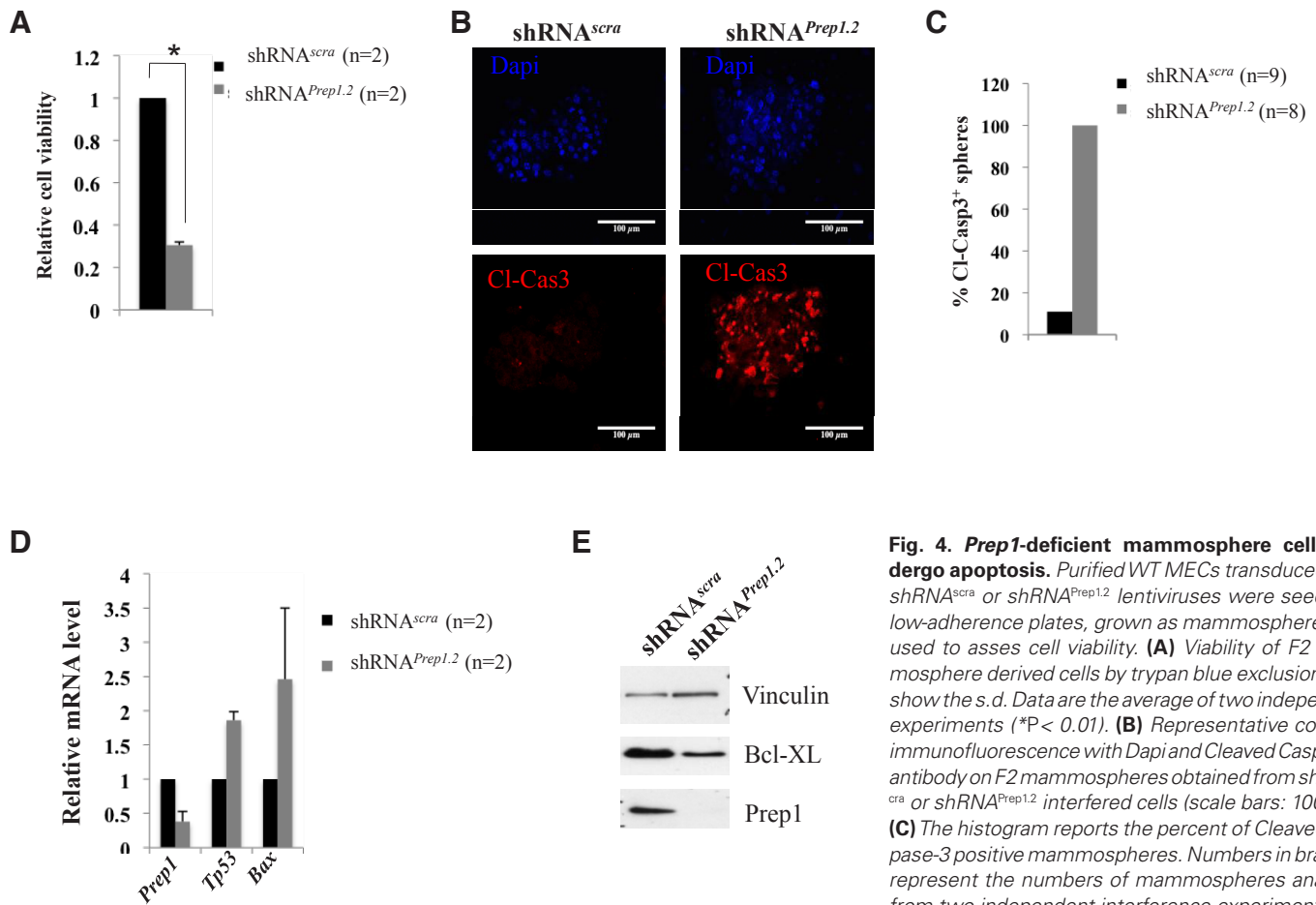


Fig. 4. *Prep1*-deficient mammosphere cells undergo apoptosis. Purified WT MECs transduced with shRNA^{scra} or shRNA^{Prep1.2} lentiviruses were seeded in low-adherence plates, grown as mammospheres and used to assess cell viability. **(A)** Viability of F2 mammosphere derived cells by trypan blue exclusion; bars show the s.d. Data are the average of two independent experiments (* $P < 0.01$). **(B)** Representative confocal immunofluorescence with Dapi and Cleaved Caspase-3 antibody on F2 mammospheres obtained from shRNA^{scra} or shRNA^{Prep1.2} interfered cells (scale bars: 100 μ m). **(C)** The histogram reports the percent of Cleaved Caspase-3 positive mammospheres. Numbers in brackets represent the numbers of mammospheres analyzed from two independent interference experiments. **(D)**

QT-PCR on total RNA from shRNA^{scra} or shRNA^{Prep1.2} F2 mammospheres; *Prep1*, *Tp53* and *Bax* mRNAs levels were evaluated. The data represent the average of two independent interference experiments. Error bars show the s.d. **(E)** Total lysate from shRNA^{scra} or shRNA^{Prep1.2} F2 mammospheres was electrophoresed on SDS-PAGE and immunoblotted with the indicated antibodies; vinculin served as a loading control.

mary gland epithelial cells in which *Prep1* was down-regulated by transduction with a specific shRNA lentiviral vector. Supplementary Fig. S4A shows examples of the effects of *Prep1* down-regulation in the two systems, whereas the graphs in Fig. 3 A,B show the quantification of the experiments. We observe a major decrease in SFE whenever *Prep1* was down-regulated. The shRNA used in Fig. 3B and Fig. S4A in the supplementary material (shRNA^{Prep1.2}) was the most efficient among the four tested (supplementary Fig. S4 B,C). A scrambled shRNA (shRNA^{scra}) served as control.

We then used a 3D Matrigel assay (O'Brien *et al.*, 2002) to test *in-vitro* the branching potential of shRNA^{scra} or shRNA^{Prep1.2} interfered mammosphere cells. In our experimental condition (see Materials and Methods), *Prep1*-interfered cells (shRNA^{Prep1.2}) show a much lower number of branches and shorter extensions (Fig. 3C) and form 6.5 fold less colonies in 3D Matrigel as compared to control cells (shRNA^{scra}) (histogram in Fig. 3C).

***Prep1* depleted MaSC/progenitor cells exhibit enhanced apoptosis**

Proliferation, apoptosis and cell migration of lineage-committed MaSC within the TEBs support mammary branching morphogenesis (Scheele *et al.*, 2017). Likely, *Prep1* deficiency might interfere with these processes.

To assess the effect of *Prep1* depletion on the proliferative behaviour of MaSC/progenitors, total RNA from F2 mammospheres, stably infected with shRNA^{scra} or shRNA^{Prep1.2} lentiviruses was retrotranscribed and used for *Ki67* mRNA amplification. The results, obtained from three independent interference experiments, reveal in *Prep1* down-regulated cells a mild, and not significant, increase in *Ki67* mRNA level (Fig. 3D).

We next evaluated the role of *Prep1* on cell survival and found that *Prep1* deficiency correlated with increased apoptosis. Indeed, cells from *Prep1* down-regulated F2 mammospheres showed impaired viability (30% by Trypan blue exclusion; histogram in Fig. 4A) due to increased apoptosis as shown by the appearance of a strong cleaved Caspase-3 immunofluorescence signal (Fig. 4B). Quantification is reported in the histogram of Fig. 4C. The apoptotic behavior of *Prep1*-down-regulated F2 cells was further confirmed by the increased expression of the pro-apoptotic *Tp53* and *Bax* mRNAs (Fig. 4D) and by the reduced level of the anti apoptotic Bcl-XL protein (Fig. 4E).

Activation of the MAPK pathway in the TEB region and acquisition of migratory behaviour by the resident cells are critical steps in mammary branching morphogenesis (Huebner *et al.*, 2016). We tested to which extent *Prep1* deficiency impacts on these processes by immunoblotting extracts from shRNA^{Prep1.2} and shRNA^{scra}

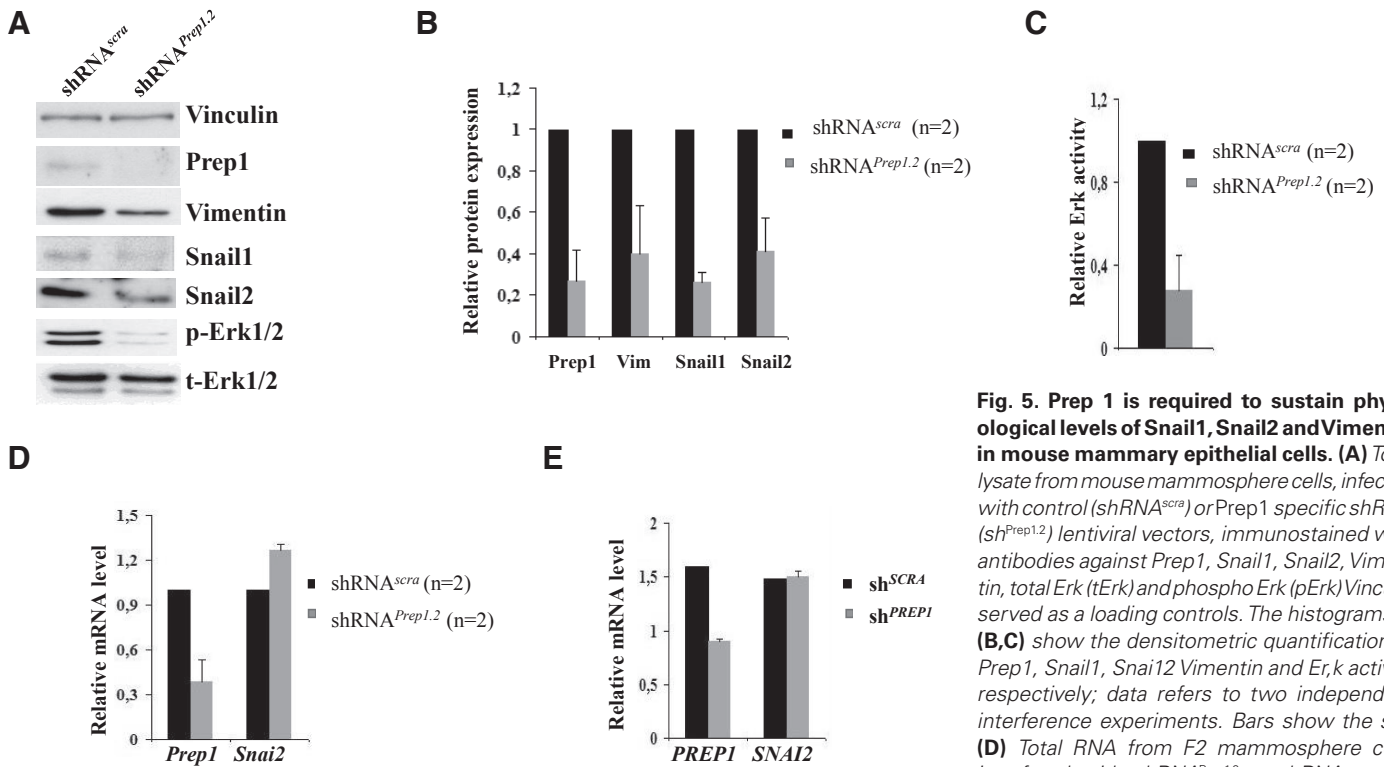


Fig. 5. Prep 1 is required to sustain physiological levels of Snail1, Snail2 and Vimentin in mouse mammary epithelial cells. (A) Total lysate from mouse mammosphere cells, infected with control (shRNA^{scra}) or Prep1 specific shRNA (sh^{Prep1.2}) lentiviral vectors, immunostained with antibodies against Prep1, Snail1, Snail2, Vimentin, total Erk (tErk) and phospho Erk (pErk). Vinculin served as a loading controls. The histograms in (B,C) show the densitometric quantification of Prep1, Snail1, Snail2, Vimentin and Erk activity respectively; data refers to two independent interference experiments. Bars show the s.d. (D) Total RNA from F2 mammosphere cells interfered with shRNA^{Prep1.2} or shRNA^{scra} viral

supernatants was extracted and cDNA used in QT-PCR to measure the levels of Prep1 and Snai2 mRNAs. Data refer to two independent experiments. Bars show the s.d. (E) Total RNA from MCF10A cells interfered with sh^{PREP1} or sh^{SCRA} viral supernatants was extracted and cDNA used in QT-PCR to measure the levels of PREP1 and SNAI2 mRNAs. Data refer to two independent experiments. Bars show the s.d.

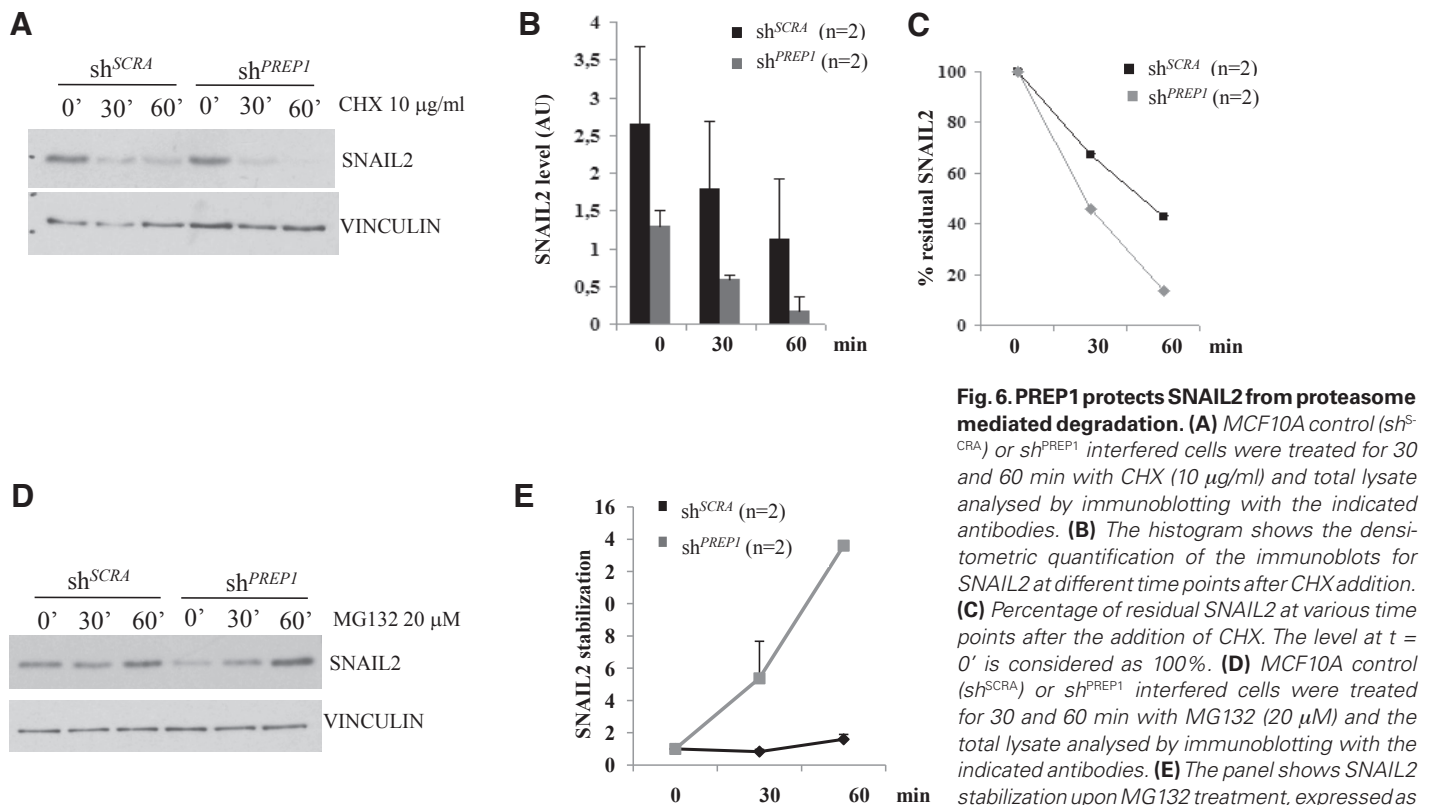


Fig. 6. PREP1 protects SNAIL2 from proteasome mediated degradation. (A) MCF10A control (sh^{SCRA}) or sh^{PREP1} interfered cells were treated for 30 and 60 min with CHX (10 μg/ml) and total lysate analysed by immunoblotting with the indicated antibodies. (B) The histogram shows the densitometric quantification of the immunoblots for SNAIL2 at different time points after CHX addition. (C) Percentage of residual SNAIL2 at various time points after the addition of CHX. The level at t = 0' is considered as 100%. (D) MCF10A control (sh^{SCRA}) or sh^{PREP1} interfered cells were treated for 30 and 60 min with MG132 (20 μM) and the total lysate analysed by immunoblotting with the indicated antibodies. (E) The panel shows SNAIL2

stabilization upon MG132 treatment, expressed as the ratio of the SNAIL2 signal measured at a given time after CHX addition with respect to that at t=0. Error bars show s.d. Data reported in panels B, C and E represent the average of two independent experiments. For both CHX and MG132 experiments, Vinculin served as loading control.

-interfered F2 mammospheres using pERK, total ERK, Snail1, Snail2 and Vimentin antibodies. We found that *Prep1* deficient cells showed attenuated Erk activity compared to control cell and a reduced Snail1, Snail2 and Vimentin level (Fig. 5 A-C). Similar results were observed in human MCF10A mammary gland cells (Soule *et al.*, 1990), in which stable *PREP1* down-regulation by a human sh^{PREP1} retrovirus, decreased ERK activity and SNAIL1, SNAIL2 and VIMENTIN signals (Fig. S5). IHC confirmed the reduced expression of Snail1 and Vimentin in mammary gland sections of 5 weeks old *Prep1*^{i/i} mice (Fig. S6).

Overall these data indicate that MAPK signalling and mediators, required for branching morphogenesis, are severely compromised in the absence of *Prep1*.

***Prep1* protects *Snail2* from proteasome mediated degradation**

Snail transcription factors are inducers of EMT and act as survival factors. In mammary branching morphogenesis *Snail2* has been reported to protect cells from p53-dependent apoptosis (Lee *et al.*, 2011). In our model of *Prep1* down-regulation we found a concomitant p53-dependent apoptosis and reduction of *Snail2* level.

As transcription factor, *Prep1* might control *Snail2* at the transcriptional level. However in both mammospheres and MCF10A models *Snail2* modulation depended on a post transcriptional mechanism since no variation in *Snai2* mRNA level was observed in interfered compared to control cells (Fig. 5 D,E).

We previously reported that *Prep1* is able to stabilize its Pbx cofactors by preventing proteasome-mediated degradation (Lon-

gobardi and Blasi, 2003). Therefore, *Prep1* might have a similar protective role also on *Snail2*. To address this possibility MCF10A cells, stably interfered with shRNA^{PREP1} or control retrovirus particles, were treated for 30' or 60' with the protein translation inhibitor cycloheximide (CHX) and the total lysate analyzed by immunoblotting using the indicated antibodies (Fig. 6A). Treatment of cells with CHX resulted in a faster SNAIL2 degradation rate in *PREP1* depleted cells as compared to the control cells, suggesting that in the mammary epithelial cells *PREP1* stabilizes SNAIL2. Quantification of SNAIL2 level and residual SNAIL2 upon treatment at different time points are reported in Fig. 6 B and C, respectively. The SNAIL2 degradation in *PREP1* interfered cells was counteracted by the proteasome inhibitor MG132 (Fig. 6D). After 30' with MG132, SNAIL2 level in *PREP1*-depleted cells was comparable to the control cells and further increased at 60'. Quantification of SNAIL2 stabilization is reported in Fig. 6E. Overall, the data suggest that *PREP1* is required to protect SNAIL2 from proteasome-mediated degradation.

***PREP1* forms complexes with SNAIL2**

To accomplish its protective function, *PREP1* might form a complex with SNAIL2. The *in-situ* proximity ligation assay (Soderberg *et al.*, 2008) on MCF10A cell can evaluate the presence of *PREP1*/*SNAIL2*-containing complexes. Indeed, in our experimental conditions, *PREP1*/*SNAIL2* co-localization dots were present in the nuclei of the cells (red dots in Fig. 7A). We confirmed this interaction by pull-down experiment using MCF10A nuclear extract and recombi-

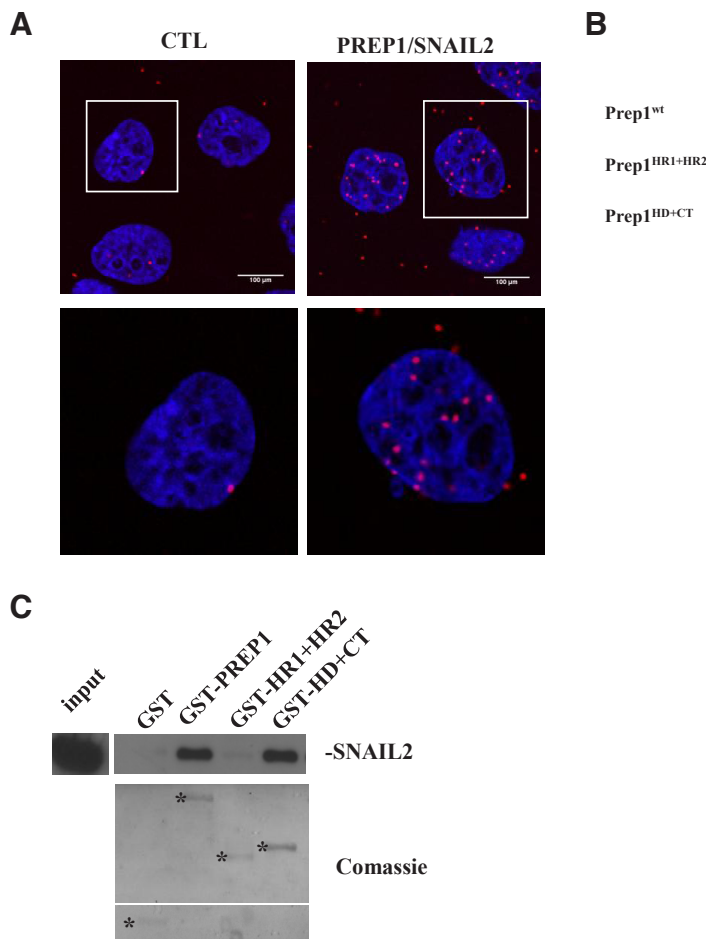


Fig. 7. *PREP1* forms complexes with *SNAIL2*. (A) Confocal images of MCF10A cells tested in proximity ligation *in-situ* assay. Top panels: *PREP1*/*SNAIL2* complexes (red dots) were visualized by staining the cells with proximity probes directed against *PREP1* and *SNAIL2*, followed by ligation and rolling circle amplification (see Methods). DAPI was used to stain the nuclei. Bottom panels: for a better evaluation of the *PREP1*/*SNAIL2* colocalization dots, (red), higher magnification of selected areas from top panels are presented. In the control, *PREP1* primary antibody was omitted in the staining procedure. Scale bars: 10 μ m. (B) Schematic representation of different *PREP1* constructs used in the pull down assay. (C) Bacterially purified GST or GST-*PREP1* constructs (asterisks in the "Coomassie" panel) were used as bait for pull down assay with MCF10A nuclear extract. The above panel shows the immunoblot with anti *SNAIL2* antibody; input represents the MCF10A nuclear extract. *SNAIL2* binds a fragment spanning residues 223-436 of *PREP1*.

nant GST-PREP1 constructs missing individual domains of PREP1 (Fig. 7B). Indeed GST-PREP1^{wt} and GST^{HD+CT} (containing only the homeodomain and the C-terminal fragment), but not GST^{HR1+HR2} (containing only the N-terminal moiety of PREP1), pulled down SNAIL2 suggesting that the HD+CT region of PREP1 contains the domain involved in SNAIL2 complex formation (Fig. 7C).

Discussion

In this work we describe, for the first time, that Prep1 transcription factor and its major partner Pbx1 are present in the mouse mammary gland and contribute to the gland's branching morphogenesis. Prep1 and Pbx1 are expressed in differentiated luminal and myoepithelial ductal cells as well as in mammospheres (Fig S1 and Fig. S3). The cytoplasmic presence of Prep1 in luminal cells is not unique. Prep1 nuclear localization appears to be regulated, for example in the early stages of the zebrafish development (De Florian et al., 2004). Its significance and the mechanisms of regulation however are still obscure, although the cytoplasmic presence of Prep1 indicates an inactive state (Berthelsen et al., 1999). *Prep1* deficiency correlates with branching defects of the differentiated cells and with the dysfunction of the stem/progenitor compartment, but not with impaired hormonal responses (Fig. 1E). Consistently, Prep1 is expressed in the mammospheres, and more precisely in the progenitors cells (Fig. 2), but genetic and shRNA-mediated ablation of *Prep1* negatively impact on both stem and progenitor cells properties. Indeed Prep1 deficient MaSC/progenitor cells show a reduced SFE (Fig. 3 A,B) and an impaired *in-vitro* branching potential (Fig. 3C). Moreover Prep1-ablated MaSC/progenitors do not properly activate MAPK signaling and are not able to express needed levels of Snail1, Snail2 and Vimentin. (Fig. 5 A-C) which are required to carry out p-EMT.

Inhibition of apoptosis, activation of migration and p-EMT are required for branching morphogenesis (Lee et al., 2011). In the mammosphere model of Prep1 deficiency, all of these branching requirements are affected. Upon suboptimal expression of Prep1, mammary cells show up-regulation of inducers (*Tp53*, *Bax*) or executors (Cl-Caspase 3) of the apoptotic response and reduced expression of the anti apoptotic Bcl-XL protein (Fig. 4). This is in line with our previous works showing a *Tp53* dependent apoptosis in *Prep1*^{-/-} mouse epiblast cells and reduction of Bcl-XL in *Prep1*^{fl/fl} mouse embryo fibroblasts (Fernandez-Diaz et al., 2010; Micali et al., 2009).

Snail proteins, and Vimentin are down-regulated in Prep1-interfered cells as well as in mammary gland sections from *Prep1* hypomorphic mice (*Prep1*^{fl/fl}) suggesting that the p-EMT program is also altered in Prep1 deficient mammary cells. Our data demonstrate that PREP1 forms complexes with SNAIL2 (Fig. 7) and that this interaction prevents the proteasome-mediated degradation of SNAIL2 (Fig. 6).

In addition to induce EMT *Snails* also act as survival factors. Overexpression of p53 and decrease of Snail2 in Prep1 deficient cells are in line with the repressive role of Snail2 over *Tp53* reported by others (Kajita et al., 2004). Snail2 binds to *Tp53* promoter and its over-expression results in *Tp53* mRNA inhibition (Kajita et al., 2004) while Snail2-interfered cells do not reduce p53 level in response to growth factors (Lee et al., 2011). We propose that in specific cell contexts and in response to specific stimuli, Prep1 forms complexes with Snail2 and regulates the transcription of

Tp53 and other target genes, mainly connected to self renewal, EMT, survival and DNA-damage. The presence of Prep1-Snail2-containing complexes in the nuclei of the cells (Fig. 7A) supports this hypothesis. Snail genes are also potent inducers of EMT and cell migration. It is reasonable that Prep1-deficient mammary epithelial cells, in which we observe a consistent and concomitant reduction in Vimentin, Snail1 and Snail2 signals, could not migrate properly. Notably, we previously reported that overexpressed PREP1 induces EMT and confers prometastatic behaviour to A549 cells (Risolino et al., 2014). Our data on MAPK activation in Prep1-deficient cells further suggest migration impairment in the branching phenotype of Prep1 deficient gland.

Prep1- and *Snai*-deficient models share some common features. Snail1 and Snail2 are involved in development. *Snai1* null embryos fail to produce mesoderm and do not gastrulate; *Snai2* null mutants are viable although they express a broad range of defects. Snails are also connected to DNA-damage response and genomic instability. Deletion of *Prep1* causes gastrulation arrest due to genomic instability (Fernandez-Diaz et al., 2010; Palmigiano et al., 2018), its down-regulation in *Prep1* hypomorphic embryos likewise causes organogenesis defects (Ferretti et al., 2006) and alteration of stem/progenitor compartments. Importantly, down-regulation or deletion of *Prep1* induce accumulation of DNA double strand breaks (Iotti et al., 2011) by affecting the timing of replication of Lamin-associated DNA (Palmigiano et al., 2018) in agreement with the development of tumors (including mammary gland tumors) in *Prep1* deficient mice and humans (Longobardi et al., 2010). Possibly, the developmental defects and the tumor-prone phenotype of Prep1 deficient models might involve also Snail proteins. This possibility is worth being investigated.

Since Prep1 is a partner of Hox proteins via the intermediate binding of Pbx1, one wonders whether the present results are somehow intertwined with a role of *Hox* genes during mammary branching morphogenesis. Available information show that *Hox* genes are involved in the development of many branching organs and *Hox* deficiency causes branching defects (Patterson et al., 2001).

Materials and Methods

Ethics statement

All mice experiments were performed in accordance with Institutional Animal Care and Use Committee of IFOM and approved by the Italian Ministry of Health (project#109/11). All animal handlings were in accordance with the guidelines established by EU (directive 2010/63/EU).

Mice and genotyping

4 to 5 weeks old C57BL/6 mice were purchased at Charles River Laboratories (Calco, LC- Italy) and housed according to institutional guidelines for 1 week before experiments were performed.

Prep1^{fl/fl} mice have been previously described (Ferretti et al., 2006). Control animal (ctl) in all the experiments using the *Prep1*^{fl/fl} strain refers to wt or heterozygous animals. *Prep1* floxed mice (*Prep1*^{flxed}; C57BL/6 background) were previously described (Iotti et al., 2012). *Prep1*^{flxed} mice (*Prep1*^{fl/fl}) were crossed with a *Prep1*^{-/-} mice (Fernandez-Diaz et al., 2010) to generate *Prep1*^{fl/-} mice. The mammary gland specific deletion was obtained by crossing *Prep1*^{fl/-} mice with transgenic SV129 *Ker5Cre* mice (Ramirez et al., 2004). Genotypes were determined by amplification of genomic DNA on tail biopsies using primers described in Fernandez-Diaz et al., (2010) for *Prep1*, whereas *Ker5* primers (Table S1 in supplementary material) were used for *Ker5*^{Cre} transgene. Residual *Prep1* expression in

Mammary Epithelial Cells-enriched fraction was evaluated by RT-PCR using *Prep1*-full primers (Table S2 in supplementary material).

Whole mounts and quantification of ductal morphogenesis

The 4th inguinal mammary glands were fixed overnight in Carnoy's II fixative and gradually rehydrated. Glands were stained with Carmine Alum over-night and cleared with Xylene. Whole-mount images were acquired using an Olimpus stereo microscope SZX16 and MetaMorph software (Molecular Devices, Sunnyvale, CA, USA). ImageJ software was used to quantify ductal morphogenesis. To quantify outgrowth, the distance of the most three longest ducts per gland was measured relative to a line tangential to the proximal lymph node in each animal. The branching points analysis was done by counting the number of bifurcations within a 200x120 pixel box; 3 boxes per one inguinal gland were analysed per mouse. To quantify TEB area, the average area of the 4 largest TEBs per whole-mount was obtained by outlining the TEB using the freehand selection tool. Statistical analysis was done by Student's t test

Histology, immunofluorescence and IHC

Tissue processing and HE staining were performed by the IFOM Pathology Unit according to standard procedures. Mammary glands immuno-stainings were performed according to standard procedure. Antigen retrieval was performed by incubating slides in 10 mM sodium citrate pH 6.0. Slides were incubated in primary antibody over night and with secondary antibody for 45 min, respectively. Sections were mounted with Eukitt (Invitrogen, Carlsbad, CA, USA). Images were collected with either a Leica TCS SP2 (confocal acquisition) or Olympus QColor 3TM digital camera and Hamamatsu Orca ER fluorescence camera and processed using ImageJ software.

Dissociation of mammary tissue and mammosphere culturing

Mammary glands from wt and *Prep1^{fl/fl}* mice were dissociated mechanically and enzymatically and single cell suspension used for mammospheres culturing as described (Tosoni *et al.*, 2012). Briefly, freshly isolated mammary glands were collected, chopped with a scissor and the tissue fragments digested for 2-3 hr in DMEM (Lonza) supplemented with Collagenase (Sigma) and Hyaluronidase (Sigma). Cell suspension was serially filtered through a 100 μ m to 20 μ m cell strainer, resuspended in PBS and residual blood cells removed by hypotonic lysis. Cells were resuspended in MEBM (Lonza) supplemented with 20 ng/ml EGF (Inalco), 20 ng/ml bFGF (Peprotech), 0,5 μ g /ml Hydrocortisone (Sigma), 5 μ g /ml insulin (Roche), 1 U Heparin (Epsclair), 2% B27 Supplement (Gibco) and plated on polyEMA (Sigma) treated plates.

PKH26 staining and FACS procedures

Single cell suspensions from mammary glands from 4-5 weeks old C57BL/6 mice were labelled with PKH26 (Sigma) according to the manufacturer instruction. Labeled cells were plated in suspension and after 5-6 days, mammospheres were harvested, dissociated mechanically and re-plated for an additional mammosphere passage. Few (5-6) days later F1 mammospheres were collected, counted, dissociated mechanically and filtered through a 40 μ m cell strainer, and subjected to either FACS analysis with a FACS Vantage SE flow cytometer (Becton & Dickinson) to yield PKH26^{pos} and PKH26^{neg} cells or used in immunofluorescence. Sorting conditions for PKH26^{pos} and PKH26^{neg} populations were described (Tosoni *et al.*, 2012) with the exception of a gate of 10⁰-10¹ for PKH26^{neg} fraction.

Lentivirus infection of primary mammary epithelial cells

Passage 1 mammospheres (F1) were collected, disgregated and single cell suspensions infected with PEG (System Biosciences)-concentrated lentivirus particles containing the following shRNAs (Open Biosystem): Scramble: ccggCAACAAGATGAAGAGCACCAACTCGAGTTGGT-GCTCTTCATCTTGTGttttg
shRNA^{Prep1.1}: ccggCCCTACAACAGGGAAATGTAAGTTCGAGTTA-CATTTCCTGTTGTAGGGttttg

shRNA^{Prep1.2}: ccggGCTTCAAGTCAACAACACTGGTTCTCGAGAACCAGTT-GTTGACTTGAAGCttttg
shRNA^{Prep1.3}: ccggGCTATCAAGATGGACAGCAAACCTCGAGTTTGCTGTC-CATCTTGATAGCttttg
shRNA^{Prep1.4}: ccggGCCATTATAGGCATCCACTACTCGAGTAGTGAT-GCCTATAATGGCttttg

Infected cells were puromycin (PAA Laboratories)-selected and either plated for *in-vitro* SFE (Sphere Forming Efficiency) and branching morphogenesis or for protein and RNA extraction.

3D matrigel assay

F1 derived mammary epithelial cells (5x10³) were suspended in 1 ml assay medium [MEBM: Ham's (1:1) supplemented with 2% FBS, 10 ng/mL EGF (Inalco), 5 μ g/mL insulin (Roche), 1 μ g/mL hydrocortisone (Sigma), 0,5 μ g/mL cholera toxin (Sigma) and 2% Matrigel (BD Bioscience)] and plated in 24 well plate. Cells were cultured for two weeks and then scored for colony numbers and morphology. A branching phenotype was defined as a sphere having at least two processes (branches) extending from its central body. Statistical analysis was done by Student's t test

Cells

MCF10A cells were cultured in DMEM/F12 (Invitrogen) supplemented with 100 ng/mL cholera toxin (Sigma-Aldrich), 0,5 μ g/mL hydrocortisone (Sigma), 10 μ g/mL human insulin (Roche), 5% horse serum (Invitrogen) and 20 ng/mL EGF (Inalco). To obtain stable lines for *PREP1* down-regulation, MCF10A cells were infected with Sh^{SCRA} or Sh^{PREP1} retrovirus particles and selected with puromycin. The shRNAs used in this study were previously described (Iotti *et al.*, 2011). For MG132 and CHX experiments, cells were treated for 30 and 60 min and total extracts were processed for immunoblotting

Western Blots, RT-PCR and RT-qPCR Analysis

Nuclear and cytoplasmic extracts from mammary gland epithelial cells and mammospheres were obtained as previously described (Longobardi and Blasi, 2003). MCF10A and mammosphere total extract were obtained using Laemmli buffer. The antibodies used in this study are listed in Table S1 in supplementary material. Protein bands were visualized using the SuperSignal West Pico Substrate (Pierce, Rockford, IL) after incubation with HRP-conjugated anti-mouse, anti rabbit (Biorad) or anti-goat (Dako) secondary antibodies.

Isolation and purification of RNA was performed with the RNeasy Plus Mini Kit (QIAGEN GmbH, Hilden, Germany), followed by reverse transcription of total RNA with the SuperscriptTM III First Strand Synthesis System Kit (Invitrogen) according to manufacturer's instructions. The primer sequences used in this study are listed in Table S2 in the supplementary material. For QT-PCR, cDNA obtained with random hexamers (High Capacity cDNA Archive kit; Applied Biosystems) was amplified with the TaqMan Gene Expression assay (Applied Biosystems) and an ABI/Prism 7900 HT thermocycler. The probes to identify *Igf1*, *F3*, *Snai2*, *Tp53*, *Bax* and *Prep1* mRNAs were purchased by Applied Biosystem TaqMan gene expression assays (mouse; *Snai2*: Mm00441531_m1; *pKnox1*: Mm00479320_m1; *Tp53*: Mm00441964_g1; *Bax*: Mm0043050_m1; *Igf1*: Mm00439560_m1; *F3*: Mn00438855_m1). Human: *SNAI2* hs 00161904_m1; *PKNOX1*: hs 00231814_m1. GAPDH an 18S probes were used as reference genes.

In-situ proximity-ligation assay

In vivo complex formation in MCF10A cells was evaluated by Duo-Link *in situ* proximity ligation assay (Sigma) using SNAIL2 polyclonal and PREP1 monoclonal antibodies, according to manufacturer's protocol.

GST-pull down and immunoprecipitation

MCF10A nuclear extracts were obtained as previously described (Longobardi and Blasi, 2003), and used in pull down experiment. For GST-pull down experiments, 100 μ g of nuclear lysate were incubated for 1hr at 4 °C with GST and GST-PREP1 constructs (Diaz *et al.*, 2007). Complexes were

extensively washed, eluted with Laemmli buffer, separated on SDS-PAGE and immunostained with specific antibodies.

Acknowledgements

We wish to thank Dr. G. Bonizzi and Dr. L. Tosoni for technical advice and all members of the IFOM Imaging, Mouse Genetics and Histo-pathology facilities for their support. We are grateful to Dr. P.P Di Fiore. for the long discussions and scientific suggestions. FB was supported by grants from AIRC (Italian Association for Cancer Research) n. 12829, the Italian Ministry of Health (2008-1228056) and the Cariplo Foundation, 2010.

Author Contributions

EL, LS, and FP performed experiments; EL designed experiments and analyzed the data with FB; SP provided the K5Cre mice and suggestions; EL wrote the manuscript; EL and FB critically read the manuscript.

References

- AFFOLTER M, BELLUSCI S, ITOH N, SHILO B, THIERY J P AND WERB, Z. (2003) Tube or not to tube: remodeling epithelial tissues by branching morphogenesis. *Dev Cell* 4: 11-18.
- BERTHELSEN J, KILSTRUP-NIELSEN C, BLASI F, MAVILIO F AND ZAPPAVIGNA V. (1999) The subcellular localization of PBX1 and EXD proteins depends on nuclear import and export signals and is modulated by association with PREP1 and HTH. *Genes Dev* 13: 946-953.
- DE FLORIAN G, TISO N, FERRETTI E, MEYER D, BLASI F, BORTOLUSSI M AND ARGENTON F. (2004) Prep1.1 has essential genetic functions in hindbrain development and cranial neural crest cell differentiation. *Development* 131: 613-627.
- DIAZ VM, MORI S, LONGOBARDI E, MENENDEZ G, FERRAI C, KEOUGH RA, BACHI A AND BLASI F. (2007) p160 Myb-binding protein interact with Prep1 and inhibits its transcriptional activity. *Mol Cell Biol* 27: 7981-7990.
- FERNANDEZ-DIAZ LC, LAURENT A, GIRASOLI S, TURCO M, LONGOBARDI E, IOTTI G, JENKINS NA., FIORENZA MT, COPELAND NG AND BLASI F. (2010) The absence of Prep1 causes p53-dependent apoptosis of pluripotent epiblast cells. *Development* 137: 3393-3403.
- FERRETTI E, MARSHALL H, POPPER H, MACONOCHE M, KRUMLAUF R AND BLASI F. (2000) Segmental expression of Hoxb2 in r4 requires two separate sites that integrate cooperative interactions between Prep1, Pbx and Hox protein. *Development* 127: 155-166.
- FERRETTI E, VILLAESCUSA JC, DI ROSA P, FERNANDEZ-DIAZ LC, LONGOBARDI E, MAZZIERI R, MICCIO A, MICALI N, SELLERI L, FERRARI G. *et al.*, (2006) Hypomorphic mutation of the TALE gene Prep1 (*pKnox1*) causes a major reduction of Pbx and Meis proteins and a pleiotropic embryonic phenotype. *Mol Cell Biol* 26: 5650-5662.
- HUEBNER, R.J., NEUMANN, N.M. and EWALD, A.J. (2016) Mammary epithelial tubes elongate through mapk-dependent coordination of cell migration. *Development* 143: 983-993.
- IOTTI G, LONGOBARDI E, MASELLA S, DARDAEI L, DE SANTIS F, MICALI N AND BLASI F. (2011) Homeodomain transcription factor and tumor suppressor Prep1 is required to maintain genomic stability. *Proc Natl Acad Sci* 108: E314-322.
- IOTTI G, MEJETTA S, MODICA L, PENKOV D, PONZONI M, BLASI F. (2012) Reduction of Prep1 levels affect differentiation of normal and malignant B cells and accelerates Myc driven lymphomagenesis. *PLoS ONE* 7: E48353.
- KAJITA M, MCCLINIC KN AND WADE P. (2004) Aberrant Expression of the transcription factor snail and slug alters the response to genotoxic stress. *Mol. Cell Biol.* 24: 7559-7566.
- KLEINBERG DL. 1998. Role of IGF-I in normal mammary development. *Breast Canc. Res. Treat.* 47: 201-208.
- LEE KA, GJOEVSKI N, BOGHAERT E, RADISKY DC AND NELSON CM. (2011) Snai1, Snai2, and E47 promote mammary epithelial branching morphogenesis. *EMBO J* 30: 2662-2674.
- LONGOBARDI E AND BLASI F. (2003) Overexpression of PREP-1 in F9 teratocarcinoma cells leads to a functionally relevant increase of PBX-2 by preventing its degradation. *J Biol Chem* 278: 39235-39241.
- LONGOBARDI E, IOTTI G, DI ROSA P, MEIETTA S, NUCIFORO P, PONZONI M, DOGLIONI C, CANIATTI M, BIANCHI F, DI FIORE PP *et al.*, (2010) The homeodomain transcription factor Prep1 gene (*pKnox1*) is a haploinsufficient tumor suppressor in man and mice. *Mol Oncol* 4: 226-234.
- LONGOBARDI E, PENKOV D, MATEOS D, DE FLORIAN G, TORRES M AND BLASI F. (2014) Biochemistry of the TALE transcription factors PREP, MEIS and PBX in vertebrates. *Dev Dyn.* 243: 59-75.
- MICALI N, FERRAI C, FERNANDEZ-DIAZ LC, BLASI F AND CRIPPA PM. (2009) Prep1 directly regulates the intrinsic apoptotic pathway by controlling Bcl-X_L levels. *Mol Cell Biol* 29: 1143-1151.
- O'BRIEN LE, ZEGERS MM AND MOSTOV, KE. (2002) Opinion: Building epithelial architecture: insights from three-dimensional culture models. *Nat Rev Mol Cell Biol* 3: 531-537.
- PAINE IS AND LEWIS MT. (2017) The terminal End Bud: the little Engine that Could. *J Mammary Gland Biol Neoplasia* 22: 93-108.
- PALMIGIANO A, SANTANIELLO F, CERUTTI A, PENKOV D, PURUSHOTHAMAN D, MAKHIJA E, LUZI L, DI FAGAGNA FD, PELICCI PG, SHIVASHANKAR V, DELLINO GI, BLASI F. 2018. *Sci. Rep* 16: 3198.
- PATTERSON LT, PEMBAUR M, POTTER SS, 2001. Hoxa11 and Hoxd11 regulate branching morphogenesis of the ureteric bud in the developing kidney. *Development* 128: 2153-2161.
- PECE S, TOSONI D, CONFALONIERI S, MAZZAROL G, VECCHI M, RONZONI S, BERNARD L, VIALE G, PELICCI PG, DI FIORE PP. (2010) Biological and molecular heterogeneity of breast cancer correlates with their cancer stem cell content. *Cell* 140: 62-73.
- PENKOV D, MATEOS SM, FERNANDEZ-DIAZ LC, ROSELLO CA, TORROJA C, SANCHEZ-CABO F, WARNATZ HJ, SULTAN M, YASPO ML, GABRIELI A *et al.*, (2013) Analysis of the DNA-Binding Profile and Function of TALE Homeoproteins Reveals Their Specialization and Specific Interactions with Hox Genes/Proteins. *Cell Reports* 25: 1321-1333.
- RAMIREZ A, PAGE A, GANDARILLAS A, ZANET J, PIBRE S, VIDAL M, TUSELL L, GENESCA A, WHITAKER DA, MELTON DW *et al.*, (2004) A keratin K5Cre transgenic line appropriate for tissue-specific or generalized cre-mediated recombination. *Genesis* 39: 52-57.
- RISOLINO M, MANDIAN, IAVARONE F, DARDAEI L, LONGOBARDI E, FERNANDEZ S, TALOTTA F, BIANCHI F, PISATI F, SPAGGIARI L *et al.*, (2014) Transcription factor PREP1 induces EMT and metastasis by controlling the TGF- β -SMAD3 pathway in non-small cell lung adenocarcinoma. *Proc Nat Acad. Sci. USA* 111: e3775-e3784.
- SCHEELE CLGJ, HANNEZO E, MURARO MJ, ZOMER A, LANGEDIJK NSM, VAN OUDENAARDENA, SIMONS BD & VAN RHEENEN J. (2017) Identity and dynamics of the mammary stem cells during branching morphogenesis. *Nature* 542: 313-317.
- SELLERI L, DEPEW MJ, JACOBS Y, CHANDA SK, TSANG KY, CHEAH KS, RUBENSTEIN JL, O'GORMAN S AND CLEARY ML. (2001) Requirement for Pbx1 in skeletal patterning and programming chondrocyte proliferation and differentiation. *Development* 128: 3543-3557.
- SHAW FL, HARRISON H, SPENCE K, ABLETT PM, SIMOES BM, FARNIE G, CLARKE RB. (2012) A detailed Mammosphere Assay Protocol for the quantification of Breast Stem Cell Activity. *J Mammary Gland Biol. Neoplasia*.17: 111-7.
- SODERBERG O, LEUCHOWIUS KJ, GULLBERG M, JARVIUS M, WEIBRECHT I, LARSSON LG AND LANDERGEN U. (2008) Characterizing proteins and their interactions in cells and tissues using the *in situ* proximity ligation assay. *Methods* 45: 227-232.
- SOULE HD, MALONEY TM, WOLMAN SR, PETERSON WD, BRENZ R, MCGRATH CM, RUSSO J, PAULEY RG, JONES RF AND BROOKS SC. (1990) Isolation and characterization of a spontaneously immortalized human breast epithelial cell line, MCF10A. *Cancer Res* 50: 6075-6086.
- STINGL J, EIREW P, RICKESTON I, SHACKLETON M, VAILLANT F, CHOI D, LI HI AND EAVES C.J. (2006) Purification and unique properties of mammary epithelial stem cells. *Nature* 439: 993-997.
- TOSONI D, DI FIORE PP AND PECE S. (2012) Functional purification of human and mouse mammary stem cell. *Methods Mol Biol* 916: 59-79.

Further Related Reading, published previously in the *Int. J. Dev. Biol.*

Prolactin stimulation affects the stem cell-dependent mammary repopulating ability of embryonic mammary anlagen

Jiazhe Song, Fangrong Ding, Song Li, Siying Peng, Yixiang Zhu and Kai Xue

Int. J. Dev. Biol. (2018) 62: 623-629

<https://doi.org/10.1387/ijdb.180109kx>

An immunohistochemical analysis of Rab27B distribution in fetal and adult tissue

An Hendrix, Kathleen Lambein, Wendy Westbroek, Miguel C. Seabra, Veronique Cocquyt, Patrick Pauwels, Marc Bracke, Christian Gespach and Olivier De Wever

Int. J. Dev. Biol. (2012) 56: 363-368

<https://doi.org/10.1387/ijdb.120008ah>

Exosome signaling in mammary gland development and cancer

An Hendrix and Alistair N. Hume

Int. J. Dev. Biol. (2011) 55: 879-887

<https://doi.org/10.1387/ijdb.113391ah>

Recent insights into the effect of natural and environmental estrogens on mammary development and carcinogenesis

Vassiliki Pelekanou and Guy Leclercq

Int. J. Dev. Biol. (2011) 55: 869-878

<https://doi.org/10.1387/ijdb.113369vp>

Non-steroidal anti-inflammatory drugs target the pro-tumorigenic extracellular matrix of the postpartum mammary gland

Jenean O'Brien, Kirk Hansen, Dalit Barkan, Jeffrey Green and Pepper Schedin

Int. J. Dev. Biol. (2011) 55: 745-755

<https://doi.org/10.1387/ijdb.113379jo>

Ecosystems of invasion and metastasis in mammary morphogenesis and cancer

Marc Mareel and Susana Constantino

Int. J. Dev. Biol. (2011) 55: 671-684

<https://doi.org/10.1387/ijdb.113386mm>

Developmental and cancer research on the mammary gland nowadays

Marc Bracke and Olivier De Wever

Int. J. Dev. Biol. (2011) 55: 667-669

<https://doi.org/10.1387/ijdb.113421mb>



5 yr ISI Impact Factor (2016) = 2.421

